

## Magnetic susceptibility of doped quantum dots: interplay between binding energy and noise

Anuja Ghosh<sup>1</sup> , Sekh Md. Arif<sup>1</sup> , Manas Ghosh<sup>1,\*</sup> <sup>1</sup>Department of Chemistry, Physical Chemistry Section, Visva-Bharati University, Santiniketan, Birbhum 731 235, West Bengal, India\*corresponding author e-mail address: [pcmg77@rediffmail.com](mailto:pcmg77@rediffmail.com) | Scopus ID [8258661600](https://orcid.org/0000-0001-8258-6616)

## ABSTRACT

Current work focuses on realizing how the interaction between *binding energy* (BE) and *noise* influences the *magnetic susceptibility* ( $\chi$ ) of doped *GaAs* quantum dot (QD). The system is exposed to *Gaussian white* noise and the dopant is also characterized by a Gaussian function. The work also highlights the role of the pathway via which noise may operate in the system. We have found that it is the multiplicative noise that alters the  $\chi$  profile significantly from that of a noise-free atmosphere. However, additive noise does not change the  $\chi$  profile from that under noise-free state to any meaningful size. Often multiplicative noise induces paramagnetism in the system which otherwise shows diamagnetism. And the noise-BE interplay prominently determines the extent of diamagnetism displayed by the system.

**Keywords:** quantum dot; impurity; magnetic susceptibility; binding energy; Gaussian white noise.

## 1. INTRODUCTION

The last few decades have come across a tremendous surge in the research related to low-dimensional semiconductor systems (LDSS) e.g. quantum wells (QWLs), quantum wires (QWRs) and quantum dots (QDs). The said upsurge has its origin in the exhibition of amplified quantum effects (relative to the bulk materials) in various physical properties of LDSS (electrical, optical, magnetic etc.) because of their nanoscale extensions. Such enhanced quantum effect often couples with the tremendous flexibility in making LDSS based devices. As a result LDSS becomes integral components of various technologically important electronic devices. Therefore, it is a purely technology-oriented aspect that makes studies on LDSS such a coveted field.

In addition to this, it is fair to accept the rich academic contributions made by the LDSS-related works which exhaustively elucidate many important concepts of quantum mechanics [1].

The intrinsic confinement potential of LDSS undergoes immediate interaction with *impurity* (*dopant*) potential as soon as the latter is incorporated into LDSS. The resultant effective confinement potential manifestly alters a number of physical properties of LDSS with respect to a dopant-free condition and the said alteration possesses enormous technological relevance. Naturally, studies on LDSS Physics, taking into account the dopant contributions, has now become ubiquitous [2-25] with some special emphasis on the optical properties of LDSS under external electric and magnetic fields [26-31].

The need for understanding the electronic magnetism in nanoscale structures along with realization of appealing physics has accentuated studies on magnetic properties of LDSS [32-39].

In these studies the applied magnetic field changes the arrangements of the energy levels in space, which, in turn, affect the performance of optoelectronic devices [40]. Apart from this, works on magnetic properties of LDSS deem importance in view of the development of spintronics, elucidation of electronic structure of LDSS [35], understanding the semiconductor-metal

transitions in LDSS [41] and so on so forth. Impurity contamination to LDSS makes its magnetic properties more delicate [42-53].

The presence of *noise* often intervenes with the performance of LDSS-based devices. There are a few routes (also called 'modes' or 'pathways') by which noise can be introduced to the system externally. However, the consequences become different depending on the nature of the pathways mentioned above. Two such modes are commonly called *additive* and *multiplicative* based on how noise couples with the system coordinates. Application of noise, therefore, changes the physical properties of the system and the size of the change is correlated with the aforesaid pathways. Investigating the role of noise on physical properties of LDSS is, therefore, a pertinent problem.

Current investigation deals with how *magnetic susceptibility* ( $\chi$ ) of 2D *GaAs* QD depends on the *binding energy* (BE) of the system taking into account the noise effect. In this context the work of Khordad [38] merits special mention. In the present study the confinement in the  $x - y$  plane is delineated by parabolic potential and a magnetic field is applied along the  $z$ -direction. Thus, the QD system studied here is subjected to a kind of lateral electrostatic confinement (parabolic) of the electron in the  $x-y$  plane. In real QDs the electrons are confined in 3-directions i.e. the carriers effectively possess a quasi-zero dimensional domain. The confinement length scales  $R^1$ ,  $R^2$ , and  $R^3$  are generally different in three spatial directions, but most often  $R^3 \ll R^1 \approx R^2$ . Whenever such QDs are modelled  $R^3$  is often taken to be approaching zero and the confinement in the other two directions is delineated by a potential  $V$  with  $V(x) \rightarrow \infty$  for  $|x| \rightarrow \infty$ ,  $x = (x^1, x^2) \in R^2$ .  $x^1$  and  $x^2$  stand for the coordinates in  $x$  and  $y$  directions, respectively. It implies that, since  $R^3$  is almost zero; the potential in the other two pertinent directions stretches up to a length which is of the order of corresponding confinement length scales [54-55]. The QD is fed with *Gaussian impurity* and simultaneously is exposed to *Gaussian white noise* introduced via

additive and multiplicative pathways (modes). Profile of  $\chi$  with change in the magnetic field strength ( $B$ ) has been monitored for different values of BE of the system with special reference to

## 2. MATERIALS AND METHODS

The Hamiltonian ( $H_0$ ) representing the system is given by:

$$H_0 = H'_0 + V_{imp} + V_{noise}. \quad (1)$$

$H'_0$  is the dopant-free Hamiltonian. We consider the presence of parabolic confinement in the  $x$ - $y$  plane, an orthogonal magnetic field and invoke effective mass approximation to obtain

$$H'_0 = \frac{1}{2m^*} \left[ -i\hbar \frac{\partial}{\partial x} - \frac{\hbar^2}{2m^*} \left( \frac{\partial^2}{\partial x^2} + \frac{\partial^2}{\partial y^2} \right) + \frac{1}{2} m^* \omega_0^2 (x^2 + y^2) \right]. \quad (2)$$

$m^*$  and  $\omega_0$  are the effective mass of the electron and the harmonic confinement frequency, respectively.  $\vec{A}$  is the vector potential given by  $A = (By, 0, 0)$ , where  $B$  is the strength of the magnetic field.  $H'_0$  may be transformed to

$$H'_0 = -\frac{\hbar^2}{2m^*} \left( \frac{\partial^2}{\partial x^2} + \frac{\partial^2}{\partial y^2} \right) + \frac{1}{2} m^* \omega_0^2 x^2 + \frac{1}{2} m^* \Omega^2 y^2 - i\hbar \frac{\partial}{\partial x} \quad (3)$$

The quantity  $\Omega (= \sqrt{\omega_0^2 + \omega_c^2})$  emerges out as the effective confinement frequency in the  $y$ -direction and  $\omega_c (= \frac{eB}{m^* c})$  represents the cyclotron frequency.

$V_{imp}$  refers to the impurity (dopant) potential and reads  $V_{imp} = V_0 e^{-\gamma[(x-x_0)^2 + (y-y_0)^2]}$ . Here  $(x_0, y_0)$ ,  $V_0$  and  $\gamma^{\frac{1}{2}}$  represent the dopant location (coordinate), dopant potential strength, and the spatial regime over which the influence of the impurity potential is distributed, respectively.

$V_{noise}$  of eqn(1) denotes the noise contribution coming from the Hamiltonian. Present work exploits Gaussian white noise characterized by zero average and spatial  $\delta$ -correlation. Noise enters the system following two separate roadways (called additive and multiplicative) which physically imply diverse extents of system-noise interaction. Mathematically, the above characteristics can be described by a function  $[f(x, y)]$  which follows a Gaussian distribution (generated by Box-Muller algorithm) as given below:

$$\langle f(x, y) \rangle = 0, \quad (4)$$

the zero average condition, and

$$\langle f(x, y) f(x', y') \rangle = 2\zeta \delta[(x, y) - (x', y')], \quad (5)$$

## 3. RESULTS

In the present work we have used  $\varepsilon = 12.4$ ,  $m^* = 0.067m_0$  ( $m_0$  is the electronic mass in vacuum),  $\hbar = 0.036$  eV,  $B = 20.0$  T,  $V_0 = 50.0$  meV,  $(x_0, y_0 = 0, 0)$  and  $\zeta$  (the noise strength) =  $1.0 \times 10^{-4}$ . These values conform to GaAs QDs.

### A. Interplay between Binding Energy and Noise.

Fig. 1a depicts the profile of  $\chi$  with the variation of magnetic field ( $B$ ) for several values of BE without any noise.

The study divulges how a change in the BE of the QD system modifies its  $\chi$  with due emphasis on the role played by noise.

the spatial  $\delta$ -correlation condition,  $\zeta$  being the noise strength. Spatial  $\delta$ -correlation means we ensure that noise is truly random in nature with no memory effect. In other words, noise at any given position in space is not at all influenced by its strength at any other position [56-57]. The additive and multiplicative modes of application of noise are given by

$$V_{noise} = \lambda_1 f(x, y), \quad (6)$$

$$V_{noise} = \lambda_2 f(x, y)(x + y), \quad (7)$$

respectively.  $\lambda_1$  and  $\lambda_2$  are two arbitrary parameters in the case of additive and multiplicative noise, respectively.

Direct product basis of the harmonic oscillator eigenfunctions has been used to generate the Hamiltonian matrix ( $H_0$ ). Afterward, ( $H_0$ ) is diagonalized to determine the energy levels and the eigenstates of the system.

The average thermal energy, thermal average magnetization and temperature-dependent susceptibility are given in the work of Khordad[38]:

$$\langle E \rangle = -\frac{1}{z} \left( \frac{\partial z}{\partial \beta} \right),$$

$$\langle M \rangle = \frac{1}{z} \sum_j \left( -\frac{\partial E_j}{\partial B} \right) e^{-\beta E_j}$$

and

$$\chi = \frac{\partial \langle M \rangle}{\partial B}, \quad (8)$$

where  $z$  is the partition function and  $\beta = \frac{1}{k_B T}$ ;  $k_B$  being the Boltzmann constant.  $z$  is the most important quantity to calculate the various thermodynamic properties of a system and is defined as [38]:

$$z = \sum_j \exp(-\beta E_j)$$

The binding energy  $E_B$  for the ground state is given by

$$E_B = E_0 - E, \quad (9)$$

where  $E$  and  $E_0$  are the ground state energies of the system with and without impurity, respectively.

effect. The plot displays that  $|\chi|$  decreases with increase in  $B$  and attains some kind of steady value at large  $B$ [51, 58-60]. The plot also reveals diamagnetic nature of the system over a range of  $B$ . Moreover, from the plot we also observe a rise in  $|\chi|$  with an increase in BE for  $B < 25$  T. However, as soon as  $B$  surpasses this threshold value it manifests an exactly opposite trend revealed through drop in  $|\chi|$  as BE increases [51, 58, 60]. As a matter of

fact a *crossing behavior*[58, 60] becomes evident in the vicinity of  $B \sim 25$  T.

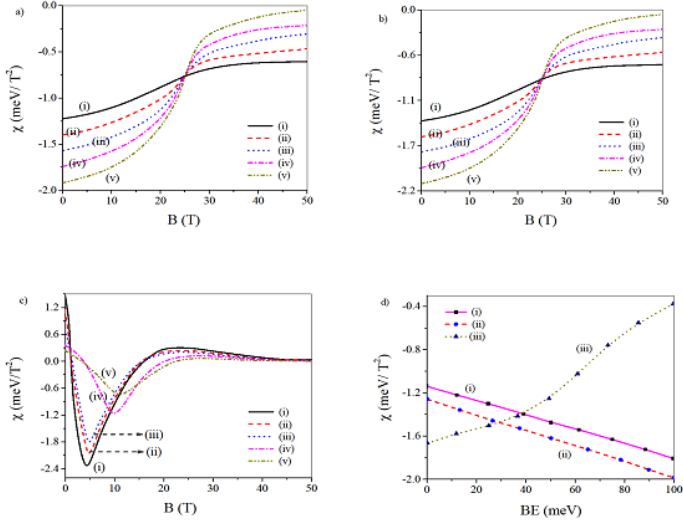


**Figure 1.** Profiles of  $\chi$  against  $B$  for different values of  $BE$ : (a) in absence of noise, (b) in presence of additive noise and (c) in presence of multiplicative noise operates. In these diagrams (i)  $BE = 0$  meV, (ii)  $BE = 25$  meV, (iii)  $BE = 50$  meV, (iv)  $BE = 75$  meV and (v)  $BE = 100$  meV. (d) Profile of  $\chi$  vs  $BE$  at  $B = 7$  T: (i) in absence of noise, (ii) in presence of additive noise and (iii) in presence of multiplicative noise.

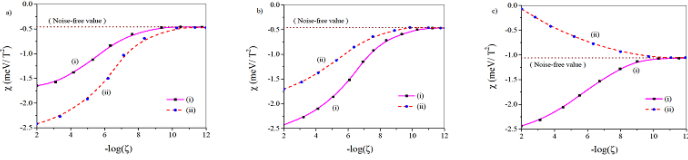


**Figure 2.** Profiles of  $\chi$  against  $-\log(\zeta)$  with noise and  $B = 5$  T: (a)  $BE = 20$  meV, (b)  $BE = 35$  meV and (c)  $BE = 50$  meV. In these diagrams (i) presence of additive noise and (ii) presence of multiplicative noise.

Fig. 1b exhibits the similar profile when additive noise is introduced and closely resembles the features of the previous noise-free plot. Thus, presence of additive noise remains indifferent towards introducing any new characteristic aspects in the  $\chi - B$  plot from that under noise-free condition; for different values of  $BE$ . The crossing behavior may have its origin in the changing effective confinement of the system, coupled with the consequent alteration in the extent of dot-impurity repulsive interaction. Up to a threshold value of  $B \sim 25$  T the system enjoys a moderate confinement. Under this situation a progressive increase in  $BE$  results into parallel enhancement of the system confinement.

However, such gradual enhancement of confinement, in turn, reduces the separation between the dot confinement center and the impurity potential. Consequent amplification in the repulsive character of the system supersedes the confinement and appears to oppose the magnetic flux more and more resulting into enhancement of diamagnetic character. When  $B$  exceeds  $\sim 25$  T, the system becomes inherently under stringent confinement. Under this situation the enhancement of  $BE$  simply reinforces the confinement of the system and increasingly suppresses its repulsive nature. Thus, the magnetic flux is opposed with gradually weakening intensity resulting into drop of  $|\chi|$ .

Remarkable change in the  $\chi - B$  profile occurs in presence of multiplicative noise [fig. 1c]. The system is now found to exhibit diamagnetic as well as paramagnetic characteristics governed by

the values of  $B$  and  $BE$ . However, for different values of  $BE$  we can frame a general appearance of the  $\chi - B$  plot when multiplicative noise operates. At the beginning, the system exhibits paramagnetism for extremely small values of  $B$  and then diamagnetism when  $B$  assumes some moderate value. The diamagnetism is observed over a rather broad range of  $B$  including some specific values of  $B$  where the diamagnetism *maximizes*. When  $B$  is increased beyond the diamagnetism zone, a mild paramagnetism is re-exhibited. Finally, at large  $B$ , the profile culminates to a nearly zero susceptibility value. Thus, even with multiplicative noise, diamagnetism seems to be more conspicuous than paramagnetism with variation of  $B$  over a considerable range. It can be further observed that the different values/ranges of  $B$  (when the system shifts from paramagnetism to diamagnetism, displays maximum diamagnetism and shows re-appearance of paramagnetism) depend on the specific values of  $BE$ . From fig. 1c it becomes evident that, with multiplicative noise, all the above phenomena generally occur at a larger value of  $B$  as  $BE$  increases. Fig. 1d delineates plot of  $\chi$  against  $BE$  at a fixed value of  $B = 7$  T in absence of noise and when additive and multiplicative noise operate. The plot helps us understand how the interplay between noise and  $BE$  can modulate  $\chi$ . As noticed earlier, at this value of  $B$  the system remains diamagnetic under all circumstances. In harmony with our previous findings, we find nearly linear increase of diamagnetism with  $BE$  in absence of noise and when additive noise is incorporated. However, application of multiplicative noise induces prominent nonlinear decline of diamagnetism as  $BE$  increases.

The effect of noise (taking into account its pathway of introduction to the system) on  $\chi$  is most effectively manifested by the plots of  $\chi$  vs  $-\log(\zeta)$  for different values of  $BE$  [figs. 2(a-c)]; where  $\zeta$  is the noise strength. From the plots it becomes evident that, quantitatively, the system exhibits three different sequences of diamagnetism guided by the introduction of noise in a given pathway and also on the domain inside which the values of  $BE$  are kept fixed. For a better comprehension, we present the following table [Table-1].

**Table 1:** Influence of noise on  $\chi$ .

Sl. No.	Range of $BE$	Sequence exhibited by diamagnetism
1.	$< 30$ meV	multiplicative $>$ additive $>$ noise-free
2.	$30$ meV to $40$ meV	additive $>$ multiplicative $>$ noise-free
3.	$> 40$ meV	additive $>$ noise-free $>$ multiplicative

Qualitatively, aboveplots also elucidate how range of  $BE$  influences the way by which diamagnetism changes as noise strength decreases. With the introduction of additive noise, diamagnetism invariably decreases with decrease in  $\zeta$  for all the different ranges of  $BE$ . However, introduction of multiplicative noise causes fall (rise) of diamagnetism as  $\zeta$  decreases for  $BE < 40$  meV ( $> 40$  meV). As expected, for both the pathways of application of noise,  $\chi$  settles to the noise-free value for very small value of the noise strength.

One of the major findings of the manuscript being that presence of multiplicative noise often induces paramagnetism in the system while additive noise does not. A look at eqns. 6 and 7 reveals that these two modes of noise interact with the system in entirely different manners. Multiplicative noise causes greater

perturbation of the system (with respect to noise-free situation) than its additive counterpart because of its more intimate coupling with the system coordinates. Close looks at eqns. (1), (6) and (7) reveal that additive noise simply adds on to the Hamiltonian without making any explicit coupling with the system coordinates whereas multiplicative noise gets directly coupled with the system coordinates. Thus, quite obviously, noise-BE interaction is also modified to a noticeable level only in the presence of

#### 4. CONCLUSIONS

The magnetic susceptibility of doped *GaAs* QD has been investigated with emphasis on role of noise and following the variation of binding energy. It has been observed that the profiles of  $\chi$  in the absence of noise and with additive noise are quite similar. However, incorporation of multiplicative noise induces discernible alteration in the profile of  $\chi$  from that under noise-free ambience. In general, the system displays diamagnetism without

multiplicative noise. Since additive noise affects the system feebly the basic diamagnetic character exhibited by the noise-free system remains nearly unchanged in presence of it. Multiplicative noise strongly affects the binding energy of the system and sometimes becomes able to convert the basic diamagnetic character of the noise-free system to paramagnetism.

noise and when additive noise operates whereas the application of multiplicative noise brings about maximization in the diamagnetic behavior of the system and often renders the system to be paramagnetic. The magnitude of diamagnetism displayed by the system reveals different trends that depend on introduction of noise in a specific route and also on the domain inside which the binding energy varies.

#### 5. REFERENCES

1. Boyacioglu, B.; Chatterjee, A. Dia- and paramagnetism and total susceptibility of *GaAs* quantum dots with Gaussian confinement. *Physica E* **2012**, *44*, 1826-1831, <https://doi.org/10.1016/j.physe.2012.05.001>.
2. Hayrapetyan, D.B.; Ohanyan, G.L.; Baghdasaryan, D.A.; HA Sarkisyan, H.A.; Baskoutas, S.; Kazaryan, E.M. Binding energy and photoionization cross-section of hydrogen-like donor impurity in strongly oblate ellipsoidal quantum dot. *Physica E* **2018**, *95*, 27-31, <https://doi.org/10.1016/j.physe.2017.09.006>.
3. Baskoutas, S.; Paspalakis, E.; Terzis, A.F. Effects of excitons in nonlinear optical rectification in semiparabolic quantum dots. *Physical Review B* **2006**, *74*, <https://doi.org/10.1103/PhysRevB.74.153306>.
4. Baskoutas, S.; Paspalakis, E.; Terzis, A.F. Electronic structure and nonlinear optical rectification in a quantum dot: effects of impurities and external electric field. *Journal of Physics: Condensed Matter* **2007**, *19*.
5. Karabulut, İ.; Atav Ü.; Şafak, H.; Tomak, M. Linear and nonlinear intersubband optical absorptions in an asymmetric rectangular quantum well. *European Physical Journal B* **2007**, *55*, 283-288, <https://doi.org/10.1140/epjb/e2007-00055-1>.
6. Karabulut, İ.; Şafak, H.; Tomak, M. Nonlinear optical rectification in asymmetrical semiparabolic quantum wells. *Solid State Communications* **2015**, *135*, 735-738, <https://doi.org/10.1016/j.ssc.2005.06.001>.
7. Chen, B.; Guo, K.X.; Liu, Z.L.; Wang, R.Z.; Zheng, Y.B.; Li, B. Second-order nonlinear optical susceptibilities in asymmetric coupled quantum wells. *Journal of Physics: Condensed Matter* **2008**, *20*.
8. Xie, W. Nonlinear optical properties of a hydrogenic donor quantum dot. *Physics Letters A* **2008**, *372*, 5498-5500, <https://doi.org/10.1016/j.physleta.2008.06.059>.
9. Xie, W. Impurity effects on optical property of a spherical quantum dot in the presence of an electric field. *Physica B* **2010**, *405*, 3436-3440, <https://doi.org/10.1016/j.physb.2010.05.019>.
10. Xie, W. Optical absorptions of a negatively charged exciton in quantum dots. *Chemical Physics* **2012**, *408*, 69-74, <https://doi.org/10.1016/j.chemphys.2012.09.023>.
11. Hakimiyfard, A.; Barseghyan, M.G.; Kirakosyan, A.A. Simultaneous effects of pressure and magnetic field on intersubband optical transitions in Pöschl–Teller quantum well. *Physica E* **2009**, *41*, 1596-1599, <https://doi.org/10.1016/j.physe.2009.05.008>.
12. Rezaei, G.; Vaseghi, B.; Taghizadeh, F.; Vahdani, M.R.K.; Karimi, M.J. Intersubband optical absorption coefficient changes and refractive index changes in a two-dimensional quantum pseudodot system. *Superlattices and Microstructures* **2010**, *48*, 450-457, <https://doi.org/10.1016/j.spmi.2010.08.009>.
13. Kirak, M.; Yilmaz, S.; Şahin, M.; Genüçaslan, M. The electric field effects on the binding energies and the nonlinear optical properties of a donor impurity in a spherical quantum dot. *Journal of Applied Physics* **2011**, *109*, <https://doi.org/10.1063/1.3582137>.
14. Liang, S.; Xie, W. Effects of the hydrostatic pressure and temperature on optical properties of a hydrogenic impurity in the disc-shaped quantum dot. *Physica B* **2011**, *406*, 2224-2230, <https://doi.org/10.1016/j.physb.2011.03.035>.
15. Rezaei, G.; Vahdani, M.R.K.; Vaseghi, B. Nonlinear optical properties of a hydrogenic impurity in an ellipsoidal finite potential quantum dot. *Current Applied Physics* **2011**, *11*, 176-181, <https://doi.org/10.1016/j.cap.2010.07.002>.
16. Hassanabadi, H.; Liu, G.; Lu, L. Nonlinear optical rectification and the second-harmonic generation in semi-parabolic and semi-inverse squared quantum wells. *Solid State Communications* **2012**, *152*, 1761-1766, <https://doi.org/10.1016/j.ssc.2012.05.023>.
17. Liu, G.; Guo, K.X.; Hassanabadi, H.; Lu, L. Linear and nonlinear optical properties in a disk-shaped quantum dot with a parabolic potential plus a hyperbolic potential in a static magnetic field. *Physica B* **2012**, *407*, 3676-3682, <https://doi.org/10.1016/j.physb.2012.05.049>.
18. Şakiroğlu, S.; Ungan, F.; Yesilgul, U.; Mora-Ramos, M.E.; Duque, C.A.; Kasapoglu, E.; Sari, H.; Sökmen, I. Nonlinear optical rectification and the second and third harmonic generation in Pöschl–Teller quantum well under the intense laser field. *Physics Letters A* **2012**, *376*, 1875-1880, <https://doi.org/10.1016/j.physleta.2012.04.028>.
19. Baghrmian, H.M.; Barseghyan, M.G.; Kirakosyan, A.A.; Restrepo, R.L.; Duque, C.A. Linear and nonlinear optical absorption coefficients in *GaAs/Ga<sub>1-x</sub>Al<sub>x</sub>As* concentric double quantum rings: Effects of hydrostatic pressure and aluminum concentration. *Journal of Luminescence* **2013**, *134*, 594-599, <https://doi.org/10.1016/j.jlumin.2012.07.024>.
20. Zeng, Z.; Garoufalidis, C.S.; Terzis, A.F.; Baskoutas, S. Linear and nonlinear optical properties of *ZnO/ZnS* and *ZnS/ZnO* core shell quantum dots: Effects of shell thickness, impurity, and dielectric environment. *Journal of Applied Physics* **2013**, *114*, <https://doi.org/10.1063/1.4813094>.
21. Barseghyan, M.G.; Duque, C.A.; Niculescu, E.C.; Radu, A. Intense laser field effects on the linear and nonlinear optical

- properties in a semiconductor quantum wire with triangle cross section. *Superlattices and Microstructures* **2014**, *66*, 10-22, <https://doi.org/10.1016/j.spmi.2013.11.023>.
22. Ghazi, H.E.; Jorio, A.; Zorkani, I. Linear and nonlinear intra-conduction band optical absorption in *(In,Ga)N/GaN* spherical QD under hydrostatic pressure. *Optics Communications* **2014**, *331*, 73-76, <https://doi.org/10.1016/j.optcom.2014.05.055>.
23. Ghazi, H.E.; Jorio, A.; Zorkani, I. Pressure-dependent of linear and nonlinear optical properties of *(In,Ga)N/GaN* spherical QD. *Superlattices and Microstructures* **2014**, *71*, 211-216, <https://doi.org/10.1016/j.spmi.2014.03.046>.
24. Urgan, F.; Martínez-Orozco, J.C.; Restrepo, R.L.; Mora-Ramos, M.E.; Kasapoglu, E.; Duque, C.A. Nonlinear optical rectification and second-harmonic generation in a semi-parabolic quantum well under intense laser field: Effects of electric and magnetic fields. *Superlattices and Microstructures* **2015**, *81*, 26-33, <https://doi.org/10.1016/j.spmi.2015.01.016>.
25. Khordad, R.; Sedehi, H.R.R.; Bahramiyan H. Simultaneous Effects of Impurity and Electric Field on Entropy Behavior in Double Cone-Like Quantum Dot. *Communications in Theoretical Physics* **2018**, *69*, 95.
26. Sari, H.; Kasapoglu, E.; Şakiroğlu, S.; Yesilgul, U.; Urgan, F.; Sökmen, I. Combined effects of the intense laser field, electric and magnetic fields on the optical properties of *n*-type double  $\delta$ -doped *GaAs* quantum well. *Physica E* **2017**, *90*, 214-217, <https://doi.org/10.1016/j.physe.2017.03.030>.
27. Yesilgul, U.; Al, A.B.; Martínez-Orozco, J.C.; Restrepo, R.L.; Mora-Ramos, M.E.; Duque, C.A.; Urgan, F.; Kasapoglu, E. Linear and nonlinear optical properties in an asymmetric double quantum well under intense laser field: Effects of applied electric and magnetic fields. *Optical Materials* **2016**, *58*, 107-112, <https://doi.org/10.1016/j.optmat.2016.03.043>.
28. Bejan, D.; Stan, C.; Niculescu, E.C. Optical properties of an elliptic quantum ring: Eccentricity and electric field effects. *Optical Materials* **2018**, *78*, 207-219, <https://doi.org/10.1016/j.optmat.2018.02.008>.
29. Bejan, D.; Stan, C.; Niculescu, E.C. Effects of electric field and light polarization on the electromagnetically induced transparency in an impurity doped quantum ring. *Optical Materials* **2018**, *75*, 827-840, <https://doi.org/10.1016/j.optmat.2017.11.047>.
30. Yakar, Y.; Çakır, B.; Özmen, A. Dipole and quadrupole polarizabilities and oscillator strengths of spherical quantum dot. *Chemical Physics* **2018**, *513*, 213-220, <https://doi.org/10.1016/j.chemphys.2018.07.049>.
31. Urgan, F.; Mora-Ramos, M.E.; Barseghyan, M.G.; Pérez, L.M.; Laroze, D. Intersubband optical properties of a laser-dressed asymmetric triple quantum well nanostructure. *Physica E* **2019**, *114*, 113647, <https://doi.org/10.1016/j.physe.2019.113647>.
32. Krasny, Y.P.; Kovalenko, N.P.; Krey, U.; Jacak L. Paramagnetic-diamagnetic interplay in quantum dots for non-zero temperatures. *Journal of Physics: Condensed Matter* **2001**, *13*, 4341-4358, <https://doi.org/10.1088/0953-8984/13/19/313>.
33. Voskoboinikov, O.; Bauga, O.; Lee, C.P.; Tretyak, O. Magnetic properties of parabolic quantum dots in the presence of the spin-orbit interaction. *Journal of Applied Physics* **2003**, *94*, 5891-5895, <https://doi.org/10.1063/1.1614426>.
34. Voskoboinikov, O.; Lee, C.P. Magnetization and magnetic susceptibility of *InAs* nano-rings. *Physica E* **2004**, *20*, 278-281, <https://doi.org/10.1016/j.physe.2003.08.018>.
35. Climente, J.J.; Planelles, J.; Movilla, J.L. Magnetization of nanoscopic quantum rings and dots. *Physical Review B* **2004**, *70*, <https://doi.org/10.1103/physrevb.70.081301>.
36. Li, Y. Magnetization and magnetic susceptibility in nanoscale vertically coupled semiconductor quantum rings. *Journal of Computational Electronics* **2005**, *4*, 135-138, <https://doi.org/10.1007/s10825-005-7124-7>.
37. Çakır, B.; Yakar, Y.; Özmen A. Investigation of magnetic field effects on binding energies in spherical quantum dot with finite confinement potential. *Chemical Physics Letters* **2017**, *684*, 250-256, <https://doi.org/10.1016/j.cplett.2017.06.064>.
38. Khordad, R. Simultaneous effects of electron-electron interactions, Rashba spin-orbit interaction and magnetic field on susceptibility of quantum dots. *Journal of Magnetism and Magnetic Materials* **2018**, *449*, 510-514, <https://doi.org/10.1016/j.jmmm.2017.10.085>.
39. Yakar, Y.; Çakır, B.; Özmen A. Magnetic field effects on oscillator strength, dipole polarizability and refractive index changes in spherical quantum dot. *Chemical Physics Letters* **2018**, *708*, 138-145, <https://doi.org/10.1016/j.cplett.2018.08.010>.
40. Niculescu, E.C.; Stan, C.; Cristea, M.; Truscă, C. Magnetic-field dependence of the impurity states in a dome-shaped quantum dot. *Chemical Physics* **2017**, *493*, 32-41, <https://doi.org/10.1016/j.chemphys.2017.06.004>.
41. Peter, A.J.; Navaneethakrishnan, K. Semiconductor-metal transition in a quasi two-dimensional system. *Solid State Communications* **2001**, *120*, 393-396, [https://doi.org/10.1016/S0038-1098\(01\)00365-9](https://doi.org/10.1016/S0038-1098(01)00365-9).
42. Nithiananthi, P.; Jayakumar, K. Diamagnetic susceptibility of hydrogenic donor impurity in low-dimensional semiconducting systems. *Solid State Communications* **2006**, *137*, 427-430, <https://doi.org/10.1016/j.ssc.2005.12.025>.
43. Nithiananthi, P.; Jayakumar, K. Diamagnetic susceptibility of a hydrogenic donor in low lying excited states in a Quantum Well. *Superlattices and Microstructures* **2006**, *40*, 174-179, <https://doi.org/10.1016/j.spmi.2006.07.013>.
44. Peter, A.J.; Navaneethakrishnan, K. Metal-insulator transition in a semimagnetic parabolic quantum well. *Physica E* **2007**, *36*, 45-51, <https://doi.org/10.1016/j.physe.2006.07.046>.
45. Elagoz, S.; Amca, R.; Kutlu, S.; Sökmen I. Shallow impurity binding energy in lateral parabolic confinement under an external magnetic field. *Superlattices and Microstructures* **2008**, *44*, 802-808, <https://doi.org/10.1016/j.spmi.2008.09.001>.
46. Elagoz, S.; Başer, P.; Yahşib, U. The magnetic field dependency of hydrogenic impurity binding energy under inverse lateral parabolic potential. *Physica B* **2008**, *403*, 3879-3882, <https://doi.org/10.1016/j.physb.2008.07.025>.
47. Khordad, R.; Fathizadeh, N. Simultaneous effects of temperature and pressure on diamagnetic susceptibility of a shallow donor in a quantum antidote. *Physica B* **2012**, *407*, 1301-1305, <https://doi.org/10.1016/j.physb.2012.01.133>.
48. Safarpour, G.; Barati, M.; Moradi, M.; Davatolhagh, S.; Zamani, A. Binding energy and diamagnetic susceptibility of an on-center hydrogenic donor impurity in a spherical quantum dot placed at the center of a cylindrical nano-wire. *Superlattices and Microstructures* **2012**, *52*, 387-397, <https://doi.org/10.1016/j.spmi.2012.05.005>.
49. Safarpour, Gh.; Jamasb, A.; Dialameh, M.; Yazdanpanahi, S. The effect of hydrostatic pressure on the binding energy and diamagnetic susceptibility of a laser dressed donor impurity in a *GaAs/GaAlAs* nanowire superlattice. *Superlattices and Microstructures* **2014**, *76*, 442-452, <https://doi.org/10.1016/j.spmi.2014.10.030>.
50. Khordad, R.; Sadeghzadeh, M.A.; Jahan-Abad, A.M. Specific heat of a parabolic cylindrical quantum dot in the presence of magnetic field. *Superlattices and Microstructures* **2013**, *58*, 11-19, <https://doi.org/10.1016/j.spmi.2013.02.005>.
51. Boda, A.; Chatterjee, A. Transition energies and magnetic properties of a neutral donor complex in a Gaussian *GaAs* quantum dot. *Superlattices and Microstructures* **2016**, *97*, 268-276, <https://doi.org/10.1016/j.spmi.2016.06.009>.

52. Karaaslan, Y.; Gisi, B.; Şakiroğlu, S.; Kasapoglu, E.; Sari, H.; Sökmen, I. Electric and magnetic field modulated energy dispersion, conductivity and optical response in double quantum wire with spin-orbit interactions. *Physics Letters A* **2018**, *382*, 507-515, <https://doi.org/10.1016/j.physleta.2017.12.018>.
53. Bera, A.; Ghosh, A.; Ghosh, M. Analyzing magnetic susceptibility of impurity doped quantum dots in presence of noise. *Journal of Magnetism and Magnetic Materials* **2019**, *484*, 391-402, <https://doi.org/10.1016/j.jmmm.2019.04.005>.
54. Jacak, L.; Hawrylak, P.; Wojos, A. *Quantum Dots*. Springer-Verlag, Berlin, 1998; <https://doi.org/10.1007/978-3-642-72002-4>.
55. Chakraborty, T. *Quantum Dots-A Survey of the Properties of Artificial Atoms*. Elsevier, Amsterdam, 1999; <https://doi.org/10.1016/B978-0-444-50258-2.X5000-7>.
56. García-Ojalvo, J.; Sancho, J.M. *Noise in Spatially Extended Systems*. Springer, New York, USA, 1999; <https://doi.org/10.1007/978-1-4612-1536-3>.
57. Sancho, J.M.; Miguel, M.S.; Katz, S.L.; Gunton, J.D. Analytical and numerical studies of multiplicative noise. *Phys. Rev. A* **1982**, *26*, 1589-1609, <https://doi.org/10.1103/PhysRevA.26.1589>.
58. Boda, A.; Chatterjee, A. Effect of an external magnetic field on the binding energy, magnetic moment and susceptibility of an off-centre donor complex in a Gaussian quantum dot. *Physica B* **2014**, *448*, 244-246, <https://doi.org/10.1016/j.physb.2014.02.059>.
59. Boda, A.; Chatterjee, A. The Binding Energy and magnetic susceptibility of an off-Centre  $D^0$  donor in the presence of a magnetic field in a *GaAs* quantum dot with Gaussian confinement: an improved treatment. *Journal of Nanoscience and Nanotechnology* **2015**, *15*, 6472-6477, <https://doi.org/10.1166/jnn.2015.10900>.
60. Boda, A.; Gorre, M.; Chatterjee, A. Effect of external magnetic field on the ground state properties of  $D^-$  centres in a Gaussian quantum dot". *Superlattices and Microstructures* **2014**, *71*, 261-274, <https://doi.org/10.1016/j.spmi.2014.03.017>.

## 6. ACKNOWLEDGEMENTS

The authors A. G., S. M. A. and M. G. thank DST-FIST (Govt. of India) and UGC-SAP (Govt. of India) for support. Special thanks to Mrs. Aindrila Bera for her sincere help.



© 2020 by the authors. This article is an open access article distributed under the terms and conditions of the Creative Commons Attribution (CC BY) license (<http://creativecommons.org/licenses/by/4.0/>).